Photoperiodic encoding by the neuronal network of the suprachiasmatic nucleus

Leest, H.T. van der

Citation

Leest, H. T. van der. (2010, November 3). *Photoperiodic encoding by the neuronal network of the suprachiasmatic nucleus*. Retrieved from https://hdl.handle.net/1887/16100

CHAPTER 4

Seasonal Encoding by the Circadian Pacemaker of the SCN

VanderLeest,H.T., Houben,T., Michel,S., Deboer,T., Albus,H., Vansteensel,M.J., Block,G.D., and Meijer,J.H. (2007). Seasonal encoding by the circadian pacemaker of the SCN. **Curr. Biol.** *17*, 468-473.

Summary

The circadian pacemaker of the suprachiasmatic nucleus (SCN) functions as a seasonal clock through its ability to encode day length (Mrugala et al., 2000; Sumova et al., 2003; Schaap et al., 2003; Nuesslein-Hildesheim et al., 2000; Messager et al., 1999; Sumova et al., 1995). To investigate the mechanism by which SCN neurons code for day length, we housed mice under long (LD 16:8) and short (LD 8:16) photoperiods. Electrophysiological recordings of multiunit activity (MUA) in the SCN of freely moving mice revealed broad activity profiles in long days and compressed activity profiles in short days. The patterns remained consistent after release of the mice in constant darkness. Recordings of MUA in acutely prepared hypothalamic slices showed similar differences between the SCN electrical activity patterns *in vitro* in long and short days. *In vitro* recordings of neuronal subpopulations revealed that the width of the MUA activity profiles was determined by the distribution of phases of contributing units within the SCN. The subpopulation patterns displayed a significantly broader distribution in long days than in short days. Long-term recordings of single-unit activity revealed short durations of elevated activity in both short and long days (3.48 and 3.85h, respectively). The data indicate that coding for day length involves plasticity within SCN neuronal networks in which the phase distribution of oscillating neurons carries information on the photoperiod's duration.

Results and Discussion

In vivo Multiunit Recordings

Exposure to long and short photoperiods had marked effects on the circadian pattern of wheel-running activity in mice (Figure 4.1). In short days, animals showed long durations of nocturnal activity, whereas in long days, animals exhibited short intervals of activity. These data agree with previous reports on the wheel-running activity of mice under long or short photoperiods (Pittendrigh and Daan, 1976b; Refinetti, 2002). *In vivo* multiunit recordings from SCN neurons of freely moving mice in long and short days revealed high discharge rates during the day and low levels during the night, for both photoperiods (Figures 4.2A and 4.2B). During exposure to light-dark (LD) cycles, the mean duration of elevated electrical activity, calculated as the width of the peak at half of its amplitude, was 10.48 ± 0.61h (n = 4) in short days and 14.88 ± 1.13h (n = 4) in long days. Peak times during the last two days in LD occurred at "external time"
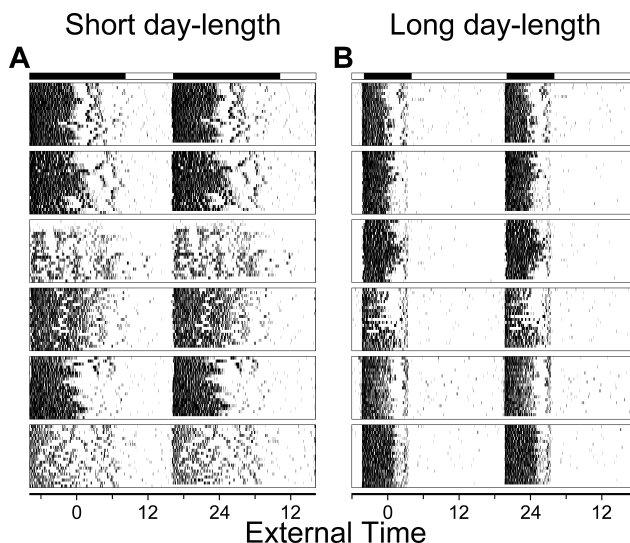

Figure 4.1

Double Plotted Actograms of Mice Kept under a Short Day and Long Day Light Regime

The light regime is plotted on top as a bar with the black part representing the dark period. The animals showed expanded (A) or compressed (B) durations of activity in accordance with the light dark cycle.

(ExT) 11.45 ± 0.27h (n = 4) for the short-day group and at ExT 15.68 ± 0.65h (n = 4) for the long-day group (ExT 12 = midday). In both photoperiods, these peaks occurred 4 - 5h before lights off. Half-maximum values were reached 5.89 ± 0.31h (n = 4) and 10.29 ± 1.34h (n = 4) before the peak time and 4.60 ± 0.28h (n = 4) and 4.60 ± 0.57h (n = 4) after the peak time in short and long days, respectively. The results show that the expansion in electrical activity is asymmetrical with respect to the peak times, and lengthening in long days occurs during the rising phase of the electrical activity pattern.
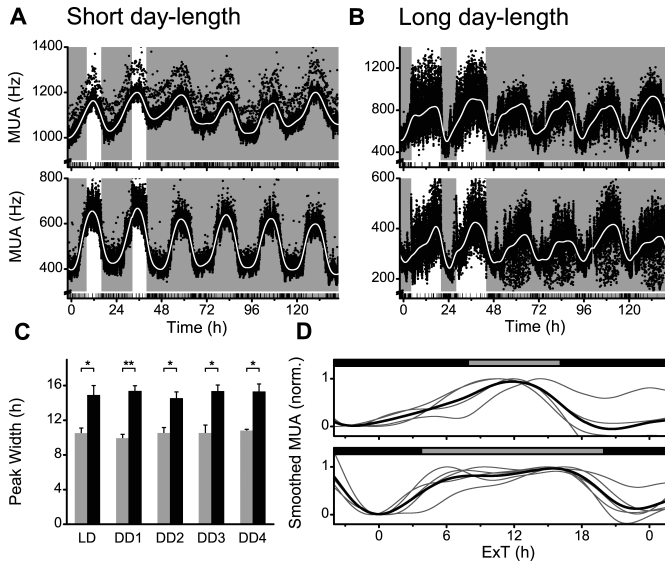

Figure 4.2

SCN Neuronal Activity Measured *In vivo* after Entrainment to Short or Long Day Photoperiods

(A and B) Two typical examples of recordings showing the last two days of multiunit electrical activity of freely moving mice in an LD 8:16 (A) or LD 16:8 (B) photoperiod and the first 4 subsequent days in DD (dark indicated by gray background). Individual data points represent 10s epochs. Smoothed data are indicated by a white line. Drinking activity is shown at the bottom of each plot.

(C) Mean width of the peak, measured at half maximum electrical activity (± SEM) during LD and the first 4 days in DD. Gray bars represent data from animals kept in short day photoperiod, and black bars represent data from long day animals (short day length, n = 4, 4, 4, 4, and 2 on the consecutive days, and long day length, n = 4, 5, 5, 5, and 4 on the consecutive days). Asterisks indicate a significant peak width difference between the recordings (t-test, *p < 0.05, **p < 0.001).

(D) Smoothed waveforms of the recorded MUA on the first day in constant darkness. The x-axis represents extrapolated external time (ExT 0 = midnight, ExT 12 = midday).

The top bar indicates the prior light dark cycle, and the gray coloring represents lights on. Data are normalized by setting the first trough value to 0 and the first peak value to 1. Gray lines represent individual recordings, and black lines are the averaged waveform (short day length n = 4, long day length n = 5).
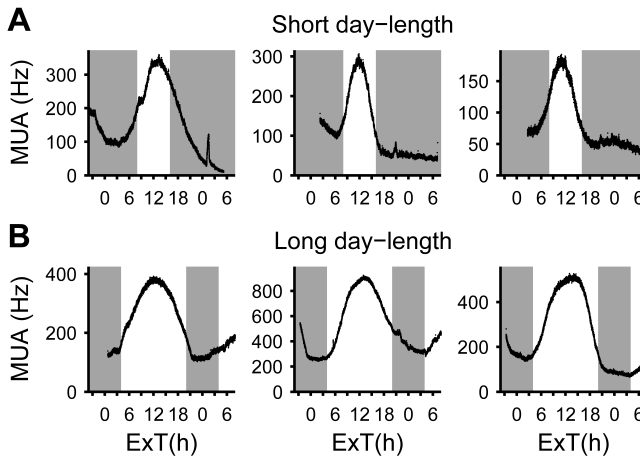
Figure 4.3

***In vitro* Multiunit Activity of Animals Housed under Short and Long Photoperiods**

Raw data traces of electrical impulse frequency, plotted per 10s. The 36h x-axis represents external time (ExT 12 = midday). The gray background represents the dark period of the previous light dark cycle. The widths of the peaks for animals in short day length (A) were narrower than those obtained in long days (B).

After the mice were released in constant darkness, the peak widths remained significantly different and stable for at least 4 days of recording, without evidence of adaptation (Figure 4.2C; two-way ANOVA, $p < 0.0001$, with post-hoc t-tests). The sustained waveform generated by the SCN (Figure 4.2D) indicates that photoperiodic information is present in the electrical output signal of the SCN *in vivo*.

In vitro Multiunit and Subpopulation Recordings

To investigate whether changes in circadian waveform are caused by a change in phase relationships among oscillating neurons, or due to photoperiod-induced changes in the neuronal activity pattern of individual cells, we explored the multiunit, subpopulation, and single-unit activities of SCN cells *in vitro*. Exposure of animals to short or long days resulted in narrow or broad multiunit discharge patterns in slices, respectively (Figure 4.3). These findings are consistent with previous *in vitro* recordings in rats and hamsters (Mrugala et al., 2000; Schaap et al., 2003) and with *in situ* measurements in the SCN of rat, hamster, and sheep (Sumova et al., 2003; Nuesslein-

Hildesheim et al., 2000; Messager et al., 1999; Sumova et al., 2002; Messager et al., 2000; Lincoln et al., 2002; Tournier et al., 2003; Carr et al., 2003; de la Iglesia et al., 2004; Johnston et al., 2005). The maximum frequency of electrical-impulse activity occurred at approximately ExT 12 for both photoperiods. Peak time occurred at ExT 11.09 ± 0.24h (n = 19) for the short-day group and at ExT 12.47 ± 0.21h (n = 24) for the long-day group. The peak times were not different between the ventral and dorsal SCN (Table 4.1) or between anterior and posterior SCN (Table 4.2); thus, this finding contrasts with the anterior-to-posterior differentiation observed *in situ* in the hamster SCN for clock-related genes per2, rev-erbα, and dbp (Hazlerigg et al., 2005).

Table 4.1
Time of Maximum Multiunit Activity *In vitro* within the Ventral and Dorsal SCN

	Ventral			Dorsal			
	PeakTime (ExT)	SEM	n	PeakTime (ExT)	SEM	n	Significance
Short day	10.72	0.36	11	11.11	0.13	13	*p* > 0.3
Long day	13.11	0.89	7	12.74	0.21	20	*p* > 0.4

The peak times were not different between the ventral and dorsal SCN (Table 4.1) or between anterior and posterior SCN (Table 4.2); thus, this finding contrasts with the anterior-to-posterior differentiation observed *in situ* in the hamster SCN for clock-related genes per2, rev-erbα, and dbp (Hazlerigg et al., 2005).

Table 4.2
Time of Maximum Multiunit Activity *In vitro* within the Anterior and Posterior SCN

	Anterior			Posterior			
	PeakTime (ExT)	SEM	n	PeakTime (ExT)	SEM	n	Significance
Short day	11.3	0.15	7	10.92	0.16	12	*p* > 0.1
Long day	12.71	0.23	12	12.87	0.26	9	*p* > 0.6

We did not observe any relation between the time of maximal firing and recording location (t-test).

The peak width of multiunit activity showed significant differences between short days (8.14 ± 0.33h, n = 20) and long days (11.76 ± 0.37h, n = 22, t-test, $p < 0.0001$). The difference in peak width between short and long days *in vitro* (4h) was consistent with the difference obtained *in vivo* (5h). This indicates that photoperiodic information is preserved in the isolated mouse SCN, *in vitro*, and this finding allows for a more detailed cellular-level investigation of the underlying mechanism.

Subpopulation activity analysis was performed by an offline analysis of spike amplitude in which we gradually increased the threshold and thereby decreased the size of the recorded unit population (Schaap et al., 2003). By including fewer neurons in the recording, the results revealed a narrower peak in electrical activity (Figure 4.4). The duration of activity for the smallest subpopulations, measured at half-maximum amplitude, was 3.72 ± 0.31h (n = 31) on short days, and 4.31 ± 0.33h (n = 34) on long days (Figure 4.5). These durations were not significantly different from one another (t-test, $p > 0.25$). A gradual increase in population size resulted in an increase in peak width (Figure 4.6). The increase in peak width occurred especially in the range of more negative, high amplitude, spike threshold levels (between -19 and -10μV).

Small subpopulations were recorded at all phases of the circadian cycle, and especially in long days, a broad distribution in phases was observed. In short days, the mean peak time, determined by a fitted Gaussian distribution, was at ExT 11.00 ± 0.04h, and the mean peak time for long days was at ExT 12.24 ± 0.23h. Although the majority of subpopulations peaked during the projected light period, a considerable number of subpopulations showed maximal activity in the projected dark (Figure 4.5). The distribution of subpopulation peak times (with the median of both groups at zero) was significantly broader in long than in short days (Quartiles, χ^2 test, $p = 0.04$). Furthermore, the distribution of the peak times was significantly different from a uniform distribution in the short days but not in the long-days condition (Rayleigh test, short days' $p = 0.0001$; long days' p

= 0.39). In addition, the Watson two-sample test comparing the distributions of the short and long days was significant ($p < 0.01$). The data indicate that differences in circadian waveform of SCN multiunit activity observed under short and long photoperiods result from the different spacing of subpopulation activity patterns.
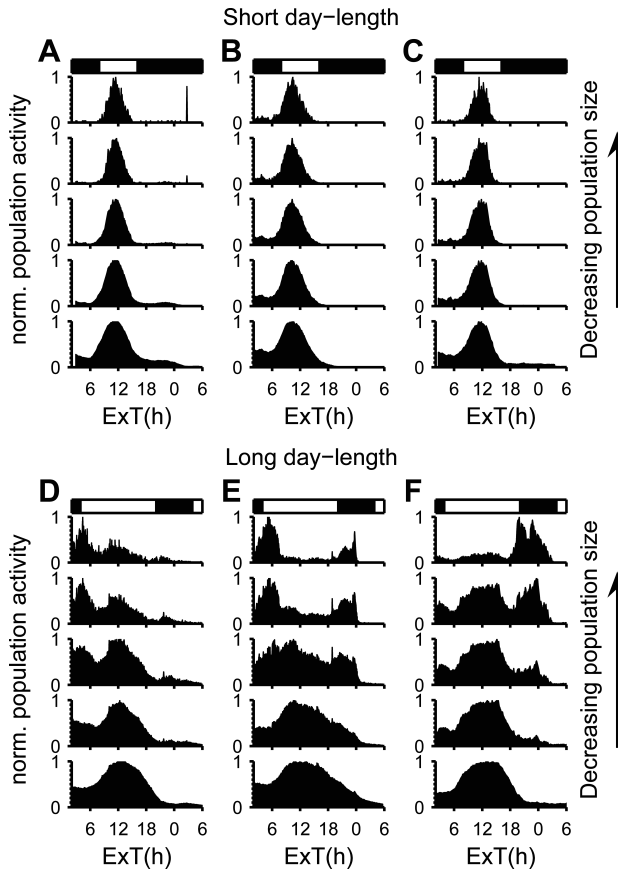

Figure 4.4

Three Examples of Normalized Cumulative Electrical Population Activity for Mice Housed under a Short Day and a Long Day Light Regime

The bars on top of each set of graphs represent the light cycle to which the animals were exposed. Population activity was calculated by a count of all threshold crossing action potentials in 2min bins over the 24h cycle, as a function of external time (ExT 12 = midday). Maximum spike frequency is normalized to 1 for enabling comparison between the graphs. The top graphs show the electrical activity pattern at near single unit level. The lower graphs contain increasingly larger populations as we lowered the threshold for action potential selection. The data show that the electrical activity pattern of the SCN is composed of out of phase oscillating neuronal populations. In long days (D F), we observed a larger phase distribution between the populations than in short days (A C).

Circadian Single-Unit Activity Patterns

Single units were distinguished with the aid of a cluster analysis of spike waveform and were verified by the additional criterion that the interval distribution must be empty at approximately time zero (i.e., units cannot fire with infinite short time intervals). When performing the single-unit analysis, we recognized that the single-unit patterns we measured may not reflect the intrinsic firing patterns of the individual neurons such as the signals recorded in dispersed cell cultures (Welsh et al., 1995; Honma et al., 1998; Herzog et al., 2004) but, rather, are the functional patterns of neurons interacting within the network. In short days, we recorded 26 single units (out of 21 slices) and in long days, 26 units (out of 18 slices). The analysis of most recordings yielded one single unit, but in some cases (seven short-day and five long-day recordings) two to three units were distinguishable in the same recording with waveform and interval characteristics (Figure 4.7). The peak times of the single-unit patterns occurred at various phases of the circadian cycle (Figure 4.8). In short as well as long days, single-unit patterns were broader during the day than during the night (Figure 4.8). Some neurons displayed regular firing patterns (n = 6 out of 26, both in long and short photoperiods). The mean duration of single-unit activity was 3.48 ± 0.29h (n = 26) on short days and 3.85 ± 0.40h (n = 26) on long days (Figure 4.8 and Figure 4.9) with no significant difference (t-test, $p > 0.4$). Single-cell recordings of mPer1 gene expression in cultured mouse SCN at the molecular level (Quintero et al., 2003; Yamaguchi et al., 2003) have shown phase differences, which could be changed by light input (Quintero et al., 2003). Narrow single-unit electrical activity patterns have been described for the SCN of rat and mouse that were kept in 12:12h LD conditions (Schaap et al., 2003; Brown et al., 2005). For different photoperiods, however, single-cell recordings have not been performed.
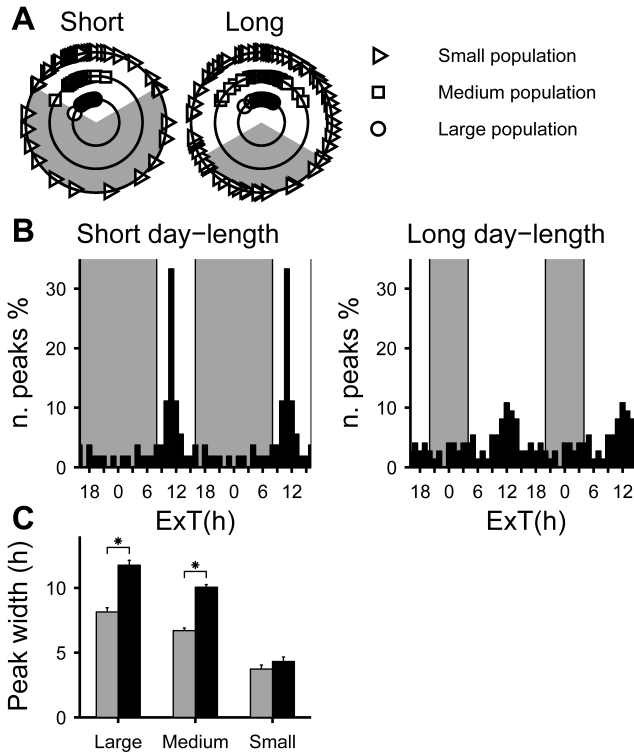
Figure 4.5

Differences in Distribution of Large, Medium, and Small Population Peak Times in SCN Neuronal Activity

Circular 24h plots of the distribution of peak times in electrical activity at the multiunit population level (inner circle, large population of about 600 units), medium population level (middle circle, about 250 neurons), and small population level (outer circle, five neurons or less).

(A) The circles are centered with midday at the top, and the gray part represents the dark. The peak times at the small population level are widely distributed.

(B) Double plotted histogram of SCN neuronal subpopulation activity peak times in short and long day length. The x-axis represents external time. The percentage of populations that peak around the middle of the day (ExT 12) is greater under short days than under long days.

(C) Bar graph showing the width (± SEM) of the activity peaks in short (shown in gray) and in long days (shown in black) for large, medium, and small populations. Asterisks indicate significance (t-test, $p < 0.0001$).

We now show that single units are active at all phases of the circadian cycle and that activity waveforms of individual units do not compress or decompress significantly in short and long days. The presence of neuronal activity during the night is consistent with previous recordings in which sampling of electrical activity for brief periods of time revealed night-time activity (Gillette et al., 1993).
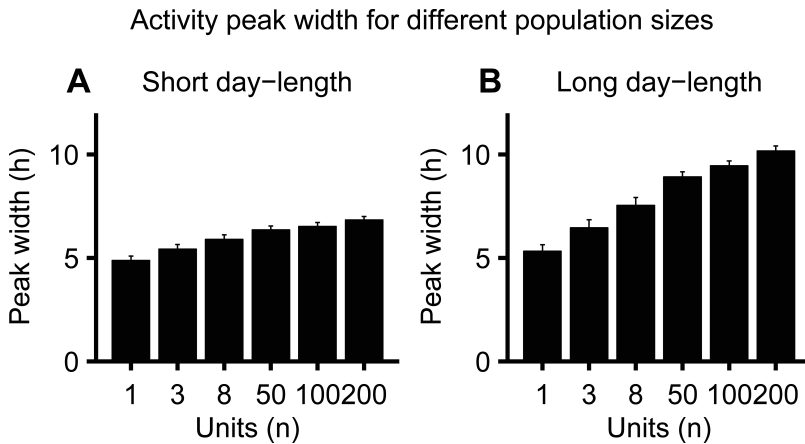
Activity peak width for different population sizes

Figure 4.6

Peak Widths for Different Estimated Population Sizes

In both day lengths the spike threshold levels were set at -19, -15, -13, -10, -9, and -8μV, respectively. These threshold levels corresponded roughly to the following number of neurons: < 1, ~3, ~8, ~50, ~100, and ~200. The number of units contributing to the signal was determined by a calculation of the area under the single unit activity curve (Figure 4.8) and the area under the subpopulation activity patterns. In short days, the increase in width caused by the inclusion of more neurons is relatively small (A), whereas in long day length, the increase in width of the peak is large (B). The data indicate that phase distribution of neuronal populations provides a mechanism to code for day length.

Although small differences in the width of the single-unit activity pattern in short and long days are not significant, they may exist. Simulation studies, however, have shown that small differences are insufficient to account for 4 - 5h changes in multiunit peak width (Rohling et al., 2006b).

Furthermore, we cannot rule out that other parameters such as clock gene expression or membrane potential show differences between short and long days. However, we should emphasize the fact that electrical-impulse activity is a major output of the clock (Schwartz et al., 1987); i.e., we strongly suspect that this is the information that is transmitted to downstream processes that would translate photoperiod information into changes in physiology and behavior.
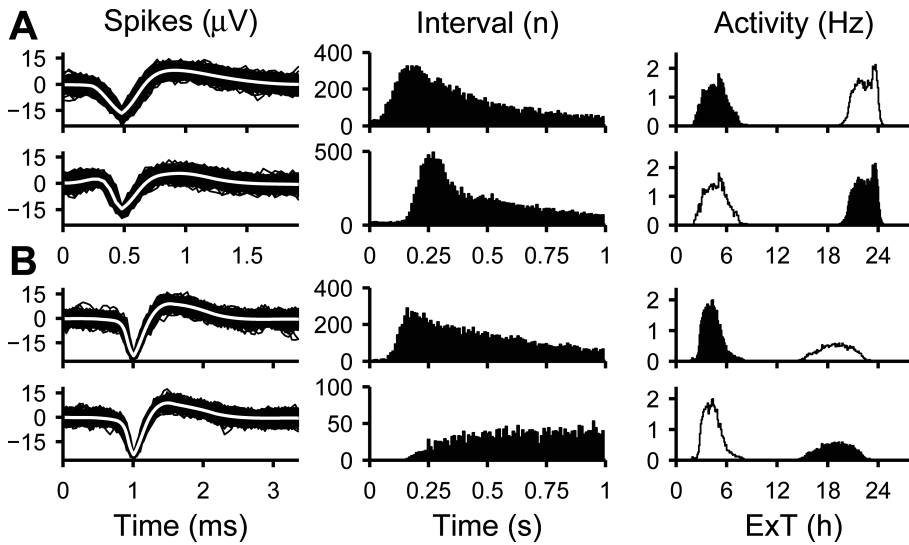
Figure 4.7

Distinct Activity Patterns of Two Single Units in One Recording

Action potential waveforms, their corresponding interspike interval histograms, and circadian activity pattern, as a function of external time, are shown in black. The secondary circadian activity pattern was recorded in the same experiment.

A) Two units were separable by their spike waveform and reflect the activity pattern of two single units.

B) Two units showed different interval characteristics but were not separable by spike waveform. The difference in interval distribution suggests that these bimodal patterns reflect the activity pattern of two different neurons or that one neuron showed a combination of its intrinsic discharge pattern at one phase and a driven pattern at another phase

Based on the single-unit activity patterns obtained in this study, it can be calculated that our smallest subpopulations consisted of less than five neurons (Figures 4.6 and 4.8). This calculation is based on the area under the subpopulation activity curve and the area of the mean single-unit activity pattern in short and long days, respectively (Figure 4.6). Most of the increase in peak width occurs when neuronal populations are increased from about 1 to 50 neurons (Figure 4.6). With 50 neurons, approximately 75% of the full peak width is obtained, both in short and in long days, and a further raise in population size resulted only in small increments in peak width. This leads us to conclude that relatively small groups of SCN neurons can carry substantial information on day length.

The *in vivo* recordings of SCN activity suggest that the phase distribution remains stable for some time even in the absence of

photic information. This corresponds with behavioral aftereffects observed in mice after exposure to different photoperiods (Pittendrigh and Daan, 1976b; Refinetti, 2002). It will be interesting to investigate whether recently identified coupling mechanisms such as VIP receptors or electrical synapses (Colwell et al., 2003; Long et al., 2005; Colwell, 2005; Aton et al., 2005) are involved in the regulation of phase relations between SCN neurons. In the present paper, we observed that plasticity in the phase differences between neurons is the primary mechanism encoding for day length.

Experimental Procedures

Animals and Recording of Behavioral Activity

Male black 6 (C57B/6JOlaHSD) mice (Harlan, Horst, the Netherlands) were entrained to 24h light dark (LD) cycles with either long (16h) or short (8h) days. The animals were housed separately with food and water ad libitum. The cages were equipped with a running wheel for recording locomotor activity of the animals in 1 min intervals. Entrainment to short and long photoperiods for less than 30 days did not lead to consistent waveform changes in the circadian rhythm of electrical activity, either *in vivo* or *in vitro*. For that reason, all animals in this study were entrained for 30 days or longer and were 9 - 14 weeks old when taken for electrophysiological recordings. Of note, C57 mice show photoperiodic responses in their behavioral activity patterns despite their melatonin deficiency, indicating that melatonin is not involved in the regulation of wheel running activity duration (Goldman, 2001). All experiments were performed under the approval of the Animal Experiments Ethical Committee of the Leiden University Medical Center.

In vivo SCN Multiunit Recording

Recording techniques have been described in detail previously (Meijer et al., 1998; Meijer et al., 1996). In brief, tripolar stainless steel electrodes (125µm, Plastics One, Roanake, Virginia) were implanted with a stereotactical instrument in the brain of animals that were under Midazolam / Fentanyl / Fluanisone anesthesia. Under a 5° angle in the coronal plane, electrodes were aimed at the following stereotaxic coordinates: 0.46mm posterior to bregma, 0.14mm lateral to the midline, and 5.2mm ventral to the surface of the cortex (Paxinos and Franklin, 2001). Two of these electrodes (Polyimide insulated) were used for differential recordings of multiunit activity from SCN neurons. The third electrode was placed in the cortex and used as reference. After a recovery period of at least 1 week, the animals were placed in the recording chamber, where drinking

activity was monitored and stored per min. The animals were connected to the recording system with a counter balanced swivel system allowing the animals to move freely. After amplification and filtering (0.5 - 5kHz) of the signal (signal to noise ratio 3:1 to 8:1), the action potentials were detected by a window discriminator and counted electronically in 10s bins. Simultaneously, drinking activity was monitored and stored in 10s epochs. After at least 30 days in the light regime and approximately 5 days of multiunit recording in the LD cycle, the animals were released into constant darkness in order to assess the properties of the neuronal activity rhythm in the absence of light. At the end of each recording, the animals were sacrificed and the recording tip was marked with a small electrolytic current for enabling histological verification of the electrode location. The iron deposition from the electrode tip was stained blue with a potassium ferrocyanide containing fixative solution in which the brain was immersed. Only recordings where the electrode location was verified to be inside the SCN were taken into account.

In vivo Data Analysis

Multiunit activity data were smoothed with a penalized least squares algorithm (Eilers, 2003). The time of maximal activity was determined in the smoothed curve, and the peak width was determined by measurement of the width at half maximum values determined bilaterally. The peak widths for the last two cycles in LD were averaged for each photoperiod. After the mice were released into constant darkness, the peak widths were averaged per day for the first 4 days for evaluation of the stability of the SCN waveform. For obtaining an average waveform for the first day in DD, the amplitude between first trough and peak was normalized in each experiment.
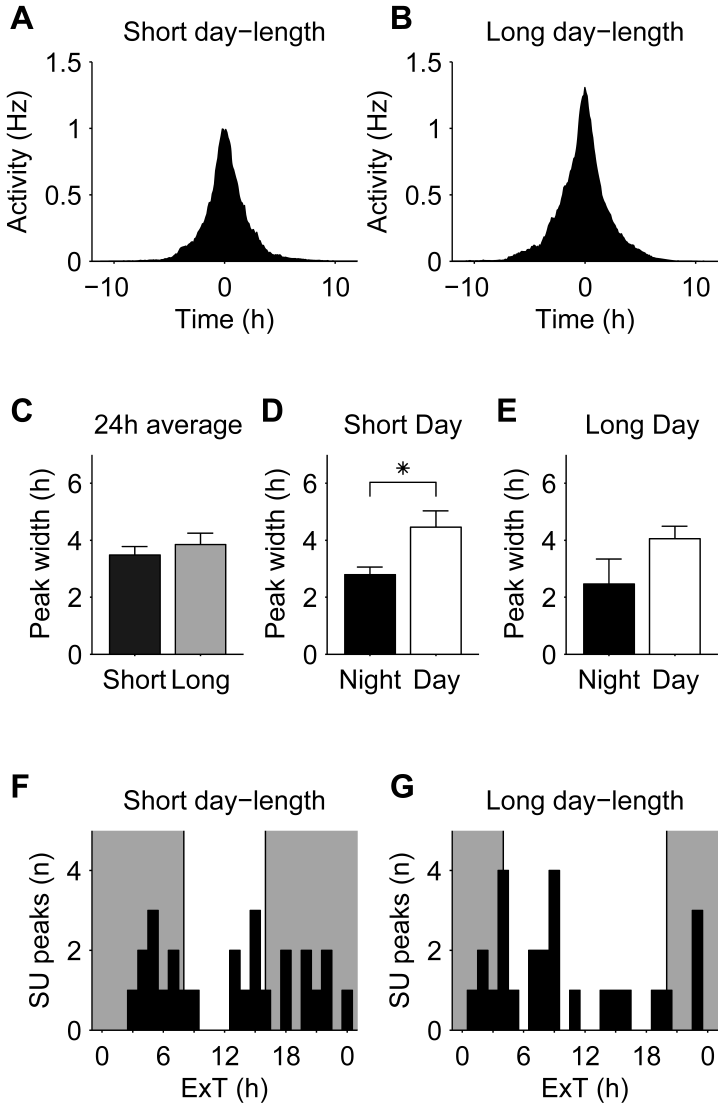
Figure 4.8

Average Single Unit Activity and Distribution of Peak Times.

(A,B) When all single unit activity peaks are centered with the peak at zero and averaged, we obtained a mean circadian activity pattern for short days (A) and for long days (B).

(C,D,E) The width of the mean single unit activity pattern (± SEM), average of the 24h circadian cycle, is shown in (C). (D) and (E) show the mean width (± SEM) of the single unit activity pattern obtained during the day and night in short and long days, respectively *p = 0.013, t-test.

(F,G) The histogram with a number of peaks in 1h bins indicates that peaks were distributed throughout the day for both short and long days.

In vitro Electrophysiology

Electrical activity rhythms of SCN neurons were recorded as described previously (Albus et al., 2002). In brief, coronal hypothalamic slices (400µm) containing the SCN were prepared from mice of the long day and short day group, 8h and 4h before lights on, respectively. Only one slice per animal was used for the recording. For the long day group, additional experiments were started at 9h before lights on (this is 1h before lights off) for excluding effects of the time of preparation on the phase and waveform of the rhythm in electrical activity. During the night, preparations were performed under dim red lighting. The slices were kept submerged in a laminar flow chamber and continuously perfused (1.5ml/min) with oxygenated artificial cerebrospinal fluid (35°C, 95% O_2, and 5% CO_2). Population and single unit electrical activity was recorded by two extracellular stationary platinum / iridium metal electrodes (50µm diameter, insulated) placed in the SCN. The signals were amplified (×10,000) and bandpass filtered (0.3 - 3kHz) by a high impedance amplifier. Action potentials were selected by a window discriminator (Neurolog system, Digitimer, Hertfordshire, UK, signal to noise ratio > 2:1) and counted electronically in 10s bins for at least 26h. In addition, the amplified signals were digitized and recorded by a data acquisition system (Power1401, Spike2 software, CED, Cambridge, UK). Amplitude and time of all action potentials crossing a threshold of approximately -6µV were recorded as a measure for subpopulation activity (see below). With thresholds above -9µV, spike templates were generated and thus isolated the activity of several units. The complete waveforms and time of occurrence of the events crossing the threshold were stored for offline analysis.
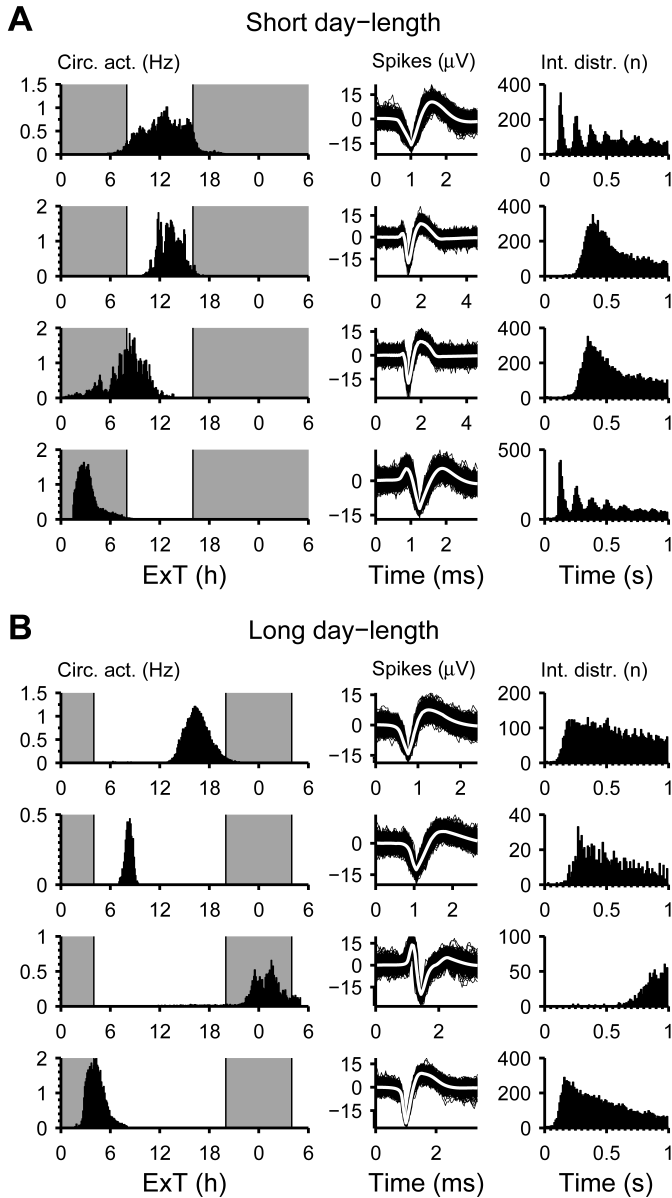
Figure 4.9

Single Units in Short and Long Day Length

Four representative examples of single unit electrical activity for animals housed under a short day (A) and long day (B) light regime. On the left, circadian activity patterns with the gray background indicating the projected dark period are shown. In the middle, the corresponding spikes with mean spike waveform (indicated by white lines) are shown. On the right, interspike interval histograms are shown. The data indicate that single units show short activity patterns in long and short days.

In vitro Data Analysis
Multiunit Activity

Multiunit activity data were smoothed with a penalized least squares algorithm (Eilers, 2003). Peak times were determined in the smoothed data and are given in external time (ExT) with ExT 0 de fined as the middle of the night. Consequently, ExT 12 is midday in both photoperiods (Daan et al., 2002). The duration of the elevated SCN activity was defined as the width of the peak at half maximum amplitude, with the values of the peak and the following trough. The location of the recording electrode was visually assessed. We distinguished between ventral and dorsal recordings and divided the rostro-caudal extend into five portions. We compared peak times of the anterior 40% with the posterior 40% and left out the middle 20% of the SCN. We also compared peak times of the ventral and dorsal 50% of the SCN.

Activity of Neuronal Subpopulations

Activity of neuronal subpopulations in the SCN was analyzed with MATLAB (The Mathworks). Amplitude data recorded from action potentials were divided into 50 equally sized bins starting at a low spike threshold level, representing a large number of neurons, to the highest threshold including only a few units (Figure 4.6). Population and subpopulation activity were smoothed and characterized by their width and peak time of the daily patterns. The width was measured in the smoothed data as the distance between the half maximum amplitude values with peak and troughs on both sides of the peak. Other values were determined as described for the multiunit data.

Single-Unit Analysis

The digitized action potential waveforms were further analyzed with MATLAB. First, the data were reduced by an increase of the thresh old. Next, a combination of principal components (PC) analysis and waveform feature selection was applied for separating the units. Clusters were generated with an expectation maximization Gaussian

model (Lewicki, 1998) with the original templates built by the Spike2 program as a starting point. In some experiments, clusters were bisected into a large number of smaller clusters and were fused together if the shape and interval of the spike would stay the same (Fee et al., 1996). This helped to reduce the number of spikes coming from multiple units and improved single unit clusters. During the mid-subjective day, the isolation of single units appeared more difficult than during the silent phases of the cycle because of the high number of spikes generated by the different neurons. The validity of single units described by the clusters was confirmed with their interspike interval (ISI) histogram, showing a lack of events in the first 50-100ms. The timing and width of single-unit activity were also calculated on smoothed data.

Statistical Analysis

The width of *in vitro* multiunit, subpopulation, and single unit activity between long and short days were compared with a two tailed independent samples t-test in SPSS and were considered to be significant if $p < 0.05$. Distribution of peak times for the small populations was compared between long day and short days with a quartile cross tabulation. We compared the middle two groups (center of the distribution) with the outer two groups (tails of the distribution). Differences in distributions were tested with a χ^2 test. We also per formed a Rayleigh test that compares the observed circular distributions with the uniform distribution in both photoperiods. In addition, we compared the two circular distributions of the short and long day conditions with the Watson two-sample test. Peak widths of *in vivo* multiunit were compared with a two way ANOVA in SPSS and then post hoc independent samples t-tests and were considered to be significant if $p < 0.05$. All values are mean ± SEM.